Phase Separation Behavior in Blends of Poly(benzimidazole) and Poly(ether imide)

D. L. VanderHart,* G. C. Campbell, and Robert M. Briber

Polymers Division, National Institute of Standards and Technology, Gaithersburg, Maryland 20899

Received February 20, 1992; Revised Manuscript Received May 1, 1992

ABSTRACT: A 50/50 blend of a poly(ether imide) (PEI) and a poly(benzimidazole) (PBI) has been studied by small-angle X-ray scattering and solid-state nuclear magnetic resonance. This blend, cast from a dimethylacetamide solution, is shown to be intimately blended on a scale of 2.5 nm. Phase separation is detectable upon annealing for 1 h at temperatures of 310 °C and above even though the DSC-determined glass transition temperature for this blend composition is 344 °C. Proton spin-diffusion concepts, along with proton multiple-pulse methods and magic angle spinning, are used to estimate the minimum domain dimensions (MDD's) in those annealed blends which display phase separation. The process of phase separation is interesting in this blend since kinetics and thermodynamics are expected to influence phase separation. The disparate T_g's (220 °C for PEI and 420 °C for PBI) suggest that the vitrification of the PBI-rich phase will arrest the growth and composition of phases in a phase-separation process. In keeping with these expectations, relatively small MDD's are observed; they range from 5 to 23 nm for annealing temperatures from 310 to 400 °C. Stoichiometric information regarding the composition of the PBI-rich phase has also been extracted from the spin-diffusion data. This composition moves closer toward a pure PBI phase as the annealing temperature is raised. Surprisingly, the composition of the PBI-rich phase has a DSC-determined T_g of about 400 °C after annealing for 1 h at only 340 °C. Thus one must be cautious about how one relates DSC-determined T_g-versus-composition data to long-term blend stability. The SAXS scattering from the phase-separated blend samples is very weak. SAXS curves showed no peaks in the small-angle region; therefore, the data were analyzed using a random-size, two-phase model from which a correlation length, ξ, was obtained. The ξ values were 3.1–4.6 times smaller than the MDD's when analysis was carried out on the same samples. This disparity, it is argued, implies that the dominant electron density fluctuations occur within the phases rather than originating from the difference in chemical composition between the phases. It is conjectured that such fluctuations could arise from stress buildup during cooling, owing to differential contraction in a bicontinuous-phase morphology. Finally, some simple solubility experiments were conducted on annealed samples. Evidence for cross-linking was seen in both the homopolymers and the blend. However, the suggestion was strong that a PEI/PBI cross-link was favored over a homopolymer cross-link. It remains an open question whether cross-linking or kinetics is responsible for arresting the growth of domains.

Introduction

Previous studies[1,2] have presented differential scanning calorimetry (DSC) data indicating that blends of a particular poly(benzimidazole) (PBI) and poly(ether imide) (PEI), solution cast from a common solvent, are single-phase materials exhibiting one composition-dependent glass transition temperature. Subsequently, in a ^{13}C NMR study,[3] a broadening and shifting of PEI carbonyl resonances in PEI/PBI blends, relative to the carbonyl resonance in neat PEI, has been taken as further evidence not only of intimate mixing but of specific interactions between PEI and PBI. Infrared evidence[2,4] garnered from changes in carbonyl and N–H bandshapes provides additional evidence for specific interactions between the PEI carbonyls and the imidazole protons. Proton spin-diffusion measurements,[5,6] similar to those which will be presented in this paper, also indicate that the blend is intimately mixed on the 2.5 nm scale. In addition, after heating above the glass transition temperature of the blend, the once-cooled blend exhibits two glass transition temperatures, thereby indicating phase separation at elevated temperature.[1,2] Blends of these materials are of interest because of the potential of obtaining materials with unique properties not available in either component alone. For example, the blends exhibit good resistance to chlorinated solvents,[1] lowered moisture uptake,[7] and a T_g intermediate between the two components.[1,2]

In this work we will investigate the distance scale and some stoichiometric aspects of phase separation using the techniques of small-angle X-ray scattering (SAXS) and nuclear magnetic resonance (NMR). Phase separation in this system is complicated by kinetic considerations originating from the disparate T_g's of the homopolymers (220 °C for PEI and 420 °C for PBI). The growth of domains at temperatures below 420 °C is expected to be strongly influenced by the mobility of the PBI-rich phase. Most of the results pertain to a 50/50 wt % PEI/PBI blend.

Experimental Section

Samples. The homopolymers used in the blends are poly[2,2′-(*m*-phenylene)-5,5′-bibenzimidazole] (PBI, Celanese Corp.)[8] and poly[2,2-bis[4-(3,4-dicarboxyphenoxy)phenyl]propane–*m*-benzenediamine] (PEI, Ultem, 1000, General Electric). Corresponding chemical structures are

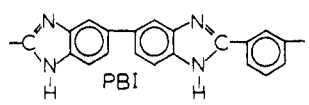

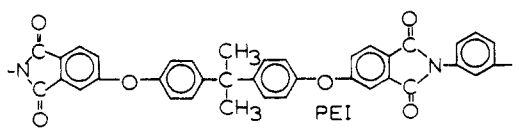

Blends were prepared by dissolving the two polymers (≈2% w/v) in dimethylacetamide (DMAc) at the desired ratio. Films of the blend were cast by pouring the solution into a Petri dish and allowing the DMAc to evaporate. The films were then washed in hot water to remove any excess DMAc; subsequently films were dried in a vacuum oven at about 100 °C. The films produced

were about 0.1–0.3 mm in thickness and were stacked to form samples on the order of 1 mm in thickness for the SAXS measurements; 2–3-mm-thick stacks of disks were used for the NMR measurements. The films were given various annealing treatments: for the 50/50 blend, samples, used for both SAXS and NMR experiments, were loaded into a long, bent, evacuated glass tube containing a small partial pressure of N_2. The sample end of the tube was inserted into a preheated furnace containing a small port; the portion of the tube outside the furnace was submerged in liquid nitrogen. Following heat treatments, especially at the higher temperatures, tiny droplets of low-volatility liquid were noted inside the tube near the exit port of the furnace. Some of this condensate was undoubtedly residual DMAc, but we also had to consider the possibility that some chemical decomposition had taken place. Heat treatment of the 75/25 PEI/PBI blend was performed in a Perkin-Elmer DSC 1B under a nitrogen atmosphere.

SAXS Measurements. The SAXS measurements were performed using a Rigaku-Denki SAXS camera with pinhole collimation and a Tennelec one-dimensional position-sensitive detector. Cu Kα X-rays were used from a rotating-anode source. The data were corrected for parasitic scattering, detector sensitivity, sample transmission, and sample thickness.

NMR Measurements. Experiments were performed at 4.7 T using a Bruker CXP-200 spectrometer equipped with a probe built by Doty Scientific. Proton spin-diffusion measurements allow us to estimate the *minimum* domain dimension (MDD) for domains of heterogeneous chemical composition in these phase-separating blends, assuming, as we do here, that the diffusion constant for this process is known. We followed closely the experimental protocol outlined in a recent paper[6] in which the tailoring of polarization gradients was discussed and illustrated for this very blend system. Briefly, these experiments are made up of four distinct periods. In the first, or so-called preparation period, gradients in polarization per spin are generated; i.e., a nonequilibrium polarization is produced with a quantization axis chosen along the static field. In the second period, whose duration is a variable spin-diffusion time, τ_{sd}, spin diffusion[9] takes place in which these polarization gradients dissipate via the extended network of proton–proton dipolar couplings in the typical polymeric solid. In the third or readout period, the extent of recovery toward internal spin equilibrium is assayed; and in the fourth period, one waits for the recovery of the Boltzmann-equilibrium polarization. Experiments incorporated the following techniques: First, multiple-pulse (MP) MREV-8[10] techniques (1.5-μs 90° pulses, 38.4-μs cycle times) were combined with magic angle spinning[11] (MAS) for both the preparation of the polarization gradient and the readout periods. Spectra incorporating both MP and MAS are referred to as CRAMPS[12] (*C*ombined *R*otation *a*nd *M*ultiple *P*ulse *S*pectroscopy) spectra. Second, initial polarization gradients were generated[13] by applying 12 MREV-8 cycles and then storing one component of the precessing magnetization alternately parallel or antiparallel to the static field with alternate addition or subtraction of data during the readout phase. The sample rotation speed was set at 4.34 kHz so that the preparation period would coincide with two rotor periods.[6] Under these circumstances this preparation produces what we refer to as a chemical-shift-based (CSB) polarization gradient; i.e., the initial polarization per spin is a sinuosidal function of the *isotropic* chemical shifts in the CRAMPS spectrum. The period of the sinusoid is about 20 ppm, depending inversely on the number of MREV-8 cycles, and the phase of the sinusoid depends on the choice of the applied radio frequency (rf). Finally, the choice of period and phase of the sinusoid in these experiments was based on enhancing the sensitivity of the *line-shape* changes to the process of spin diffusion.[6] This sensitivity is enhanced, in part, by working at smaller total integrals; a corollary is that spin-diffusion line shapes are quite dependent on the total integral. We chose to work with total integrals in the vicinity of 2% $I(M_0)$ where $I(M_0)$ is the total intensity of the CRAMPS spectrum, M_0, associated with Boltzmann-equilibrium spin polarization. Experimentally, it is difficult to maintain instrumental stability well enough to prevent a modest ($\approx$1% $I(M_0)$) drift in the total integral. Nevertheless, data analysis[6] utilizes difference polarizations, relative to the M_0 *line shape*, so that these fluctuations in the total integral contribute almost nothing to the "noise" in the data analysis. This method has sufficient sensitivity so that the dissipation of the original polarization gradient in these blends can be followed over 2.5 orders of magnitude. It is the extremely good sensitivity of this method which allows us to investigate the distance scale for phase separation in these materials.

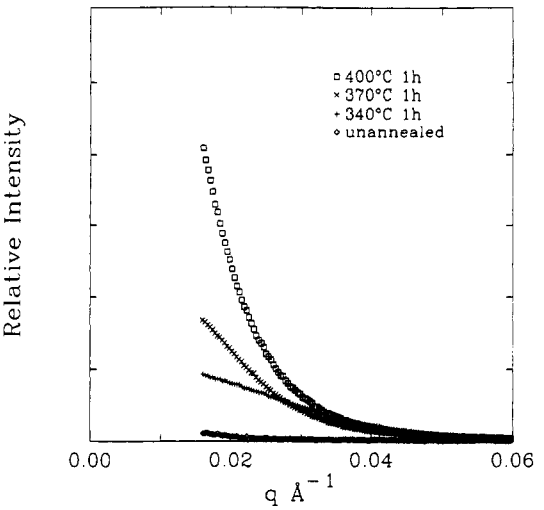

Figure 1. SAXS scattering cruves for the unannealed 50/50 PEI/PBI blend and the samples annealed for 1 h at the three highest annealing temperatures.

Results

SAXS Results. Figure 1 shows the SAXS curves for four samples derived from the 50/50 PEI/PBI blend; these are the unannealed blend, and samples annealed for 1 h at 340, 370, and 400 °C. The sample annealed at 310 °C was also examined; data (not shown) were indistinguishable from the unannealed blend data. The scattering intensity increases with increasing annealing temperature, indicating corresponding increases in the amplitude of fluctuations in the electron density and/or increases in the number of scattering sites. As expected, the unannealed blend produces almost negligible scattering, consistent with expectations based on intimate PEI/PBI mixing. Samples of 75/25 PEI/PBI were also examined, and they showed similar behavior, i.e., negligible scattering for the unannealed blend and an increasing amplitude of scattering for those samples heated to 300 and 350 °C for 24 h. It was also found that annealing samples at temperatures below 250 °C gave SAXS curves similar to the unannealed specimen.

The scattering as shown in Figure 1 was analyzed in terms of a random two-phase model characterized by a single-exponential correlation function as given in eq 1

$$c(r) = \exp(-r/\xi) \tag{1}$$

where $c(r)$ is the correlation function, r is the position vector, and ξ is the correlation length characterizing the domains in the system. The scattering from such a system was first discussed by Debye and Bueche[14] and is given in eq 2 where $I(q)$ is the scattered intensity, q is the scattering

$$I(q) = \frac{I(0)}{(1 + q^2\xi^2)^2} \tag{2}$$

vector ($q = (4\pi \sin\theta)/\lambda$ and θ is the Bragg angle), and $I(0)$ is the intensity scattered at zero angle ($q = 0$). From eq 2 it is apparent that a plot of $I(q)^{-1/2}$ versus q^2 should give a straight line, with the square root of the ratio of the slope to the intercept (at $q = 0$) being equal to the

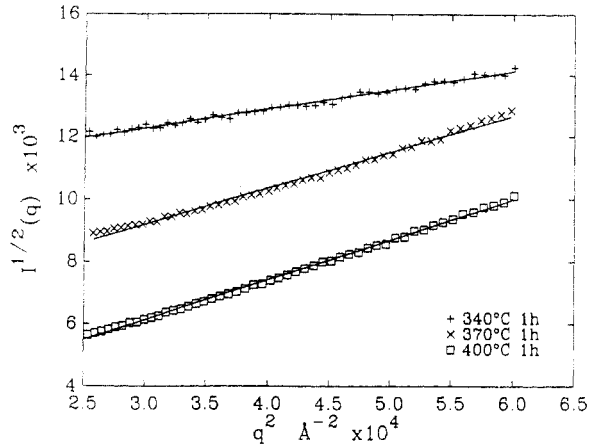

Figure 2. Plots of the inverse square root of the SAXS scattering intensity versus q^2. On the basis of eq 2, the slope of each plot together with its intercept, linearly extrapolated to $q^2 = 0$, enables one to determine the correlation length.

Table I
Comparison of SAXS Correlation Lengths (ξ) with Minimum Domain Dimensions[a] (MDD) from NMR Proton Spin-Diffusion Measurements of Heat-Treated (HT) PEI/PBI Blends

blend (PEI/PBI)	HT temp (°C)	HT time (h)	SAXS ξ (nm)	NMR MDD (nm)
50/50	none			<2.5
50/50	250	1		<2.5
50/50	280	1		<2.5
50/50	310	1		5 - 7
50/50	340	1	2.4	11.1 (1.0)
50/50	370	1	4.5	17.5 (1.4)
50/50	400	1	7.5	23.3 (1.8)
75/25	none			
75/25	300	1	3	
75/25	300	24	4	
75/25	350	0.16	5	
75/25	350	1	5.5	
75/25	350	24	6	
75/25	450	0.03	14	

[a] NMR MDD's are obtained using a lamellar model and a spin-diffusion constant of 4.6×10^{-12} cm^2/s; the corresponding overall repeat distance is twice the MDD. If the actual morphology more closely resembles a rod/matrix morphology, then the MDD is more characteristic of two orthogonal directions. It follows that the overall repeat distance will be about 1.3 times larger than that for the lamellar morphology.

correlation length. Figure 2 shows plots of this type (over the q range $0.016 < q < 0.024$ Å^{-1}) for the three 50/50 samples annealed at the indicated temperatures. Table I includes the correlation lengths determined from these plots as well as the correlation lengths for the 75/25 samples. Besides the trend of increasing SAXS correlation lengths with increasing temperatures of annealing, Table I shows that, for the 75/25 blends annealed at 350 °C, most of the development of structural inhomogeneity occurs in the first few minutes of heat treatment.

NMR Results. Figure 3 shows CRAMPS spectra of the homopolymers and the 50/50 blend where all spectra are normalized to the same total intensity. The PEI spectrum has 25% of its signal in the aliphatic region (the methyl protons) and 75% of its intensity in the aromatic region, in accordance with the chemical formula for the repeat unit. Spectra representing two PBI samples are shown to illustrate the influence of absorbed water. The undried sample has a spectrum with wings on both sides of the aromatic peak; the upfield wing disappears after drying the sample at 150 °C for 2 h. Thus, this upfield wing is associated with absorbed water, and the downfield

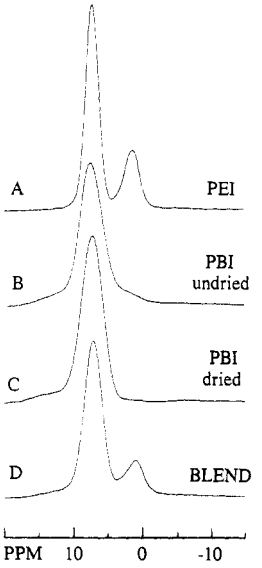

Figure 3. 200-MHz CRAMPS spectra of the indicated pure polymers and of the 50/50 PEI/PBI blend. The upfield shoulder in the undried PBI film is attributed to water; the downfield shoulder is most likely the imidazole proton. All spectra are normalized to the same total intensity. Note the wider aromatic-proton region (5–9 ppm) in PBI relative to PEI.

wing is presumably dominated by the imidazole proton whose resonance is also broadened, owing to its interaction with the bonded quadrupolar ^{14}N nucleus.[15,16] The aromatic resonance width for the PBI is broader than that for PEI. The spectrum of the 50/50 PEI/PBI blend includes features associated with the methyl resonance, an aromatic line-width intermediate between PEI and PBI, and a discernible downfield wing.

In Figure 4 we show, for illustration, CRAMPS spectra, taken in the readout period of the spin-diffusion experiment, corresponding to the sample heat treated for 1 h at 370 °C. Spin-diffusion times as well as vertical amplification factors are also given; actual total integrals of these spectra are constant at 2% $I(M_0)$. The 50-μs spectrum is a reasonable indicator of the original polarization profile; this profile is generated from the sinusoidal variation in the initial polarization per spin, P_1, indicated at the bottom of Figure 4. Initially, the aliphatic protons have near-maximum negative intensity while the aromatic line has a negative upfield side and a more-positive downfield side. There is a net excess of positive polarization so that the spin-diffusion integrals at all times will be positive. (In the absence of longitudinal relaxation effects, spin diffusion occurs at a constant total integral and the line shape evolves toward the "M_0" line shape which represents sample-wide spin equilibrium.) At τ_{sd} = 7 ms, the line shape is still very different from that of M_0, even though 7 ms is sufficient for generating internal spin equilibrium in the unannealed blend. This 7-ms line shape strongly resembles[6] that obtained for samples which are not mixed at all. In fact, this spectrum can be understood as being made up of a positive PBI and a negative PEI contribution. The structure in the aromatic region results from the narrower PEI contribution. At the 50-ms point, the PEI polarization is passing through zero; the aromatic resonance width is broad because the polarization is associated with PBI whose spectrum has that property. Finally, at 100 ms, the positive PEI polarization is evident but internal spin equilibrium has still not been attained.

Blend data like that shown in Figure 4 can be analyzed[6] and plotted against $\tau_{sd}^{1/2}$ in order to determine MDD's.

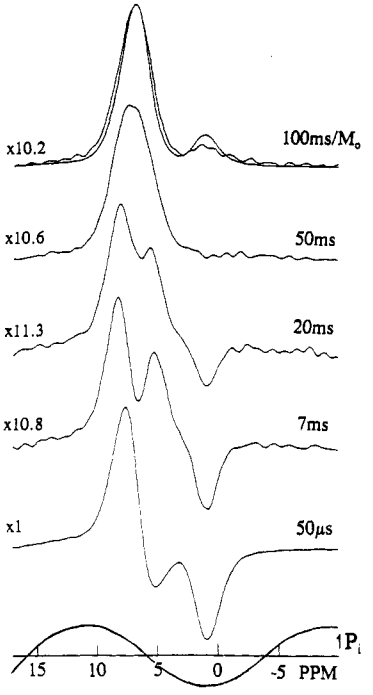

Figure 4. 200-MHz proton spin-diffusion spectra corresponding to the 50/50 PEI/PBI blend annealed for 1 h at 370 °C. The spin-diffusion times are indicated on the right; vertical amplification factors are shown on the left. Total integrals are $0.02I(M_0)$, where $I(M_0)$ is the intensity of the Boltzmann-equilibrium signal. The spin-diffusion spectrum at 50 μs shows the profile of the initial polarization; the sinusoidal modulation of the initial polarization per spin, P_i, is also shown. At the longer spin-diffusion times one can see the return of the line shape (at constant total integral) toward the shape of the equilibrium signal, M_0, shown scaled to 2% of its intensity along with the 100-ms spin-diffusion spectrum. Internal spin equilibrium, indicated by the M_0 line shape, has not quite been achieved after 100 ms of spin diffusion.

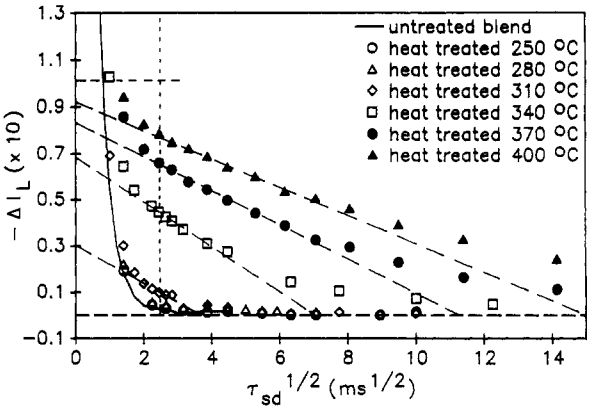

Figure 5. Plots of the deviation, $-\Delta I_L$, from internal spin equilibrium for the aliphatic protons in the indicated samples of a 50/50 PEI/PBI blend as a function of the square root of the spin-diffusion time, τ_{sd}. The dashed line at $\Delta I_L = 0$ represents internal spin equilibrium. We do not show the early time behavior between 50 μs and 1 s since all samples looked similar in this region, owing to the dominance of intramolecular spin diffusion between aromatic and aliphatic protons for PEI; typical ΔI_L values at 50 μs were −0.67. The short horizontal line at $\Delta I_L = -0.101$ indicates the extent of polarization recovery attributed only to intramolecular spin diffusion (no local mixing of PEI and PBI chains). Internal spin equilibrium in the untreated blend as well as those samples heat treated at 250 and 280 °C is achieved in 6–7 ms; this indicates good mixing on the 2.5-nm scale. A vertical dotted line is drawn corresponding to 6 ms; changes in ΔI_L beyond this time are attributed to interphase spin diffusion. Longer times are required for equilibration for those samples annealed at higher temperatures. The dashed lines drawn through the remaining data are used to calculate the domain sizes and stoichiometric quantities appearing in Tables I and II.

Figure 5 is a presentation of all of the blend data. The ordinate represents a difference polarization, i.e., a deviation from spin equilibrium. The difference is measured over the aliphatic spectral region since it is the behavior of the aliphatic resonance which will be most sensitive to the average polarization differences between PEI and PBI protons. (This follows from the fact that the intensity ratio in the aliphatic region, from ≈+4 to −1 ppm, shows the greatest deviation from unity in the homopolymer spectra of Figure 3.) Ideally we would like to integrate either the purely aliphatic-proton intensity or the purely PEI–methyl proton intensity in each of the M_0 and spin-diffusion spectra. The fact that the aromatic intensity slightly overlaps these spectral regions makes it necessary to adopt some degree of approximation in performing these integrations.

An important concept for establishing a method of data analysis is that information about domain sizes is only revealed at times longer than the time required for spin equilibration within each phase of a phase-separated morphology (≈6 ms in our case). At these longer times, each spin-diffusion spectrum will be some linear combination of undistorted spectra from each phase. For this reason, it is not very critical to the determination of MDD's what method of data analysis is chosen, so long as the data analysis can be consistently applied for all of the spectra in a given blend sample and so long as the analysis measures a quantity whose relative contributions, in the M_0 spectrum, from PEI and PBI intensities are significantly different from the corresponding PEI and PBI stoichiometric proton fractions. If this latter criterion were not satisfied, spin diffusion could occur between PEI and PBI with no change in the measured quantity.

The method of data analysis chosen in Figure 5 is the same as that discussed previously;[6] namely, integrations were performed from the "saddle-point" between the aromatic and aliphatic lines to a point exactly 5 ppm upfield. This particular integral we define to be the "aliphatic integral". This integration is truncated on both the upfield and downfield sides in order to avoid excess PBI center-band contributions on the downfield side and aliased side-band contributions, mostly from PBI, on the upfield side. The definition of the normalized polarization difference, $-\Delta I_L$, plotted on the ordinate in Figure 5 is

$$\Delta I_L = \exp(\tau_{sd}/T_1)[(I_L(\tau_{sd}) - I_L')/I_L(M_0)] \qquad (3)$$

where T_1 is the longitudinal relaxation time which is assumed uniform throughout the sample, $I_L(\tau_{sd})$ is the aliphatic integral in the spin-diffusion spectrum at τ_{sd}, I_L' is the aliphatic integral in a hypothetical spectrum having the M_0 line shape and a total integral equal to that of the spin-diffusion line shape at τ_{sd}, and $I_L(M_0)$ is the aliphatic integral in the M_0 spectrum. The exponential term compensates for signal decay resulting from T_1 processes, and the difference quantity in the numerator automatically adjusts for small changes in the total spin-diffusion integral. All experimental aliphatic integrals are measured by direct integration after proper base-line corrections and *uniform* phase corrections for all spectra. Besides these integrals, the data for a given blend sample in Figure 5 require a measurement of T_1 and the total integrals of the M_0 and spin-diffusion spectra.

From Figure 5 domain sizes will be estimated based on our ability to distinguish two time regimes, namely, the short time regime, $\tau_{sd} < 6$ ms (where spin polarization is

equilibrating within the respective monomer units and between immediately neighboring chains) and the longer time regime (where magnetization is flowing between regions of different composition). In Figure 5 the very early time behavior is not shown since this is similar for all samples. It is the isolation of the temporal behavior in the longer time regime which enables us to determine the MDD's.

In Figure 5 the solid line corresponds to the unannealed sample; this curve decays swiftly toward internal spin equilibrium at $\Delta I_L = 0$. After 2 ms of spin diffusion, the aliphatic/aromatic polarization gradient has diminished to 2% of its original size (at 50 μs, $-\Delta I_L = 0.55$), and after 7 ms, no further changes are observed. The decay profile for the untreated blend allows us to establish a conservative definition for when the "long-time" decay in phase-separated samples should be evident and measurable. We take this point to be 6 ms ($\approx$2.5 ms$^{1/2}$). Also, in consideration of the initial value of ΔI_L as well as the data fluctuations and close approach to spin equilibrium, we conclude that this method is capable of following the decay of the initially imposed aromatic/aliphatic polarization gradient over about 2.5 orders of magnitude. As the temperature of annealing is raised, the first significant deviations from the profile for the untreated sample appear at 310 °C. There is a definite extension of the curve toward longer times, relative to the profile of the untreated sample. A large relative change in the long-time decay is noted between the 310 and 340 °C data. The reported[1,2] T_g of the 50/50 blend is 344 °C; thus, this change is associated with annealing close to T_g. Especially at the three highest temperatures, the profiles break away from the fast decay associated with the untreated sample. It is this definite break which enables us to identify the longer-time decays with interphase spin diffusion and to estimate MDD's.

The procedure for estimating the MDD's from the data of Figure 5 is quite simple and unsophisticated. We assume a one-dimensional diffusion model, i.e., a lamellar model, where the MDD is the interlamellar spacing. For this lamellar model, a good estimate of the MDD is obtained by drawing a straight line, corresponding to the initial slope of the decay associated with interphase spin diffusion, and using its intercept, at $\Delta I_L = 0$, to define a characteristic time, τ_{sd}*.[17] In a highly periodic lamellar system consisting of phases with about equal fractions, this initial slope is maintained over approximately the first 65% of the decay associated with interphase spin diffusion. This time, τ_{sd}*, is then used to calculate a characteristic distance, x*, which corresponds to the root-mean-square (rms) distance that polarization can travel in a time τ_{sd}*, given that the diffusion process is described by the diffusion coefficient, D. The relationship is[17]

$$(x^{*2}) = (4/3)D\tau_{sd}^* \quad (4)$$

In the lamellar model for a 50/50 blend, x* is half the distance across either domain, assuming phase separation occurs with about equal mass fractions. Thus, the MDD will be $2x$*. For the 50/50 blend we make this same approximation. The diffusion constant, D, in eq 4 is estimated by scaling the calculated spin-diffusion constant for alkanes[18] by the cube root of the proton density;[9] for the PEI/PBI blend, this approximation gives $D = 4.6 \times 10^{-12}$ cm^2/s. In the data of Figure 5 the initial slope corresponding to interphase spin diffusion is largely obscured by intraphase spin diffusion during the first 6 ms of spin diffusion. Only when the interphase spin diffusion is slow enough that one can define a linear region between 6 ms (indicated by the vertical dotted line in Figure 5) and the time when the initial interphase polarization gradient has decayed by 50–70% can one obtain the MDD. These lines are also shown as dashed lines in Figure 5. The decay associated with the sample annealed at 310 °C is nearing completion after 6 ms and, both from an amplitude and signal-to-noise point of view, we cannot insist on ascribing linearity to the long-time decay or on extracting an MDD. We only conjecture that the mostly-obscured linear portion would have an intercept somewhere between 3.2 and 4.8 ms$^{1/2}$ and derive a corresponding range of MDD's for this sample. For annealing temperatures below 310 °C, the decay curves are indistinguishable from that of the untreated blend. Domains are thus small (<2.5 nm), just as they are in the unannealed sample.[6] The MDD's associated with all of the 50/50 blend samples are collected in Table I. Uncertainties in the MDD's, *associated only with the scatter in the data*, are given in parentheses in Table I.

We turn now to the topic of obtaining stoichiometric information from the spin-diffusion data. The intercepts at $\tau_{sd} = 0$ of the straight lines in Figure 5 are indicators of the stoichiometries of the phases since phase separation does not necessarily produce pure-homopolymer phases.[19] Qualitatively, if each phase is a mixed phase of the two homopolymers, then intraphase spin diffusion on the short time scale will bring some PEI protons into spin-diffusion contact with PBI protons. In this way the starting point, i.e., the intercept at $\tau_{sd} = 0$, for interphase spin diffusion will be reduced, relative to the intercept for phase separation into pure-homopolymer phases, commensurate with the extent of mixing.

The intercept corresponding to the pure-homopolymer phases was determined experimentally. In a spin-diffusion experiment where the sample was a physical mixture of dried PEI and PBI in the same proportions as the blend, the intercept, after corrections for the individual T_1's (400 ms for PEI, 700 ms for PBI), was $-\Delta I_L = 0.101 \pm 0.005$. A short horizontal line in Figure 5 indicates the position of this intercept.

In order to extract stoichiometric information from the actual blend samples, we first define the fractional intercept, f_i, to be the ratio of the experimental intercept to the pure-phase intercept just mentioned. In general, a knowledge of the overall blend stoichiometry and f_i is insufficient for establishing both the mass fractions and the stoichiometry of each phase in a two-phase system. One other assumption is needed. We offer two separate assumptions in order to obtain a qualitative understanding of the correspondence between intercepts and stoichiometries. Each of these assumptions is predicated on the simplifying claim that the proton fractions of PEI and PBI in the blend are both 0.5 (actually 0.51 and 0.49 in a blend with a 50/50 stoichiometry by weight). The first assumption is that thermodynamically, at these high annealing temperatures, PEI and PBI want to phase separate into nearly pure phases; however, vitrification of the PBI-rich phase arrests the further loss of PEI. Thus, the assumption is that one will get a pure-PEI phase and a mixed phase whose PEI content is closely related to the annealing temperature via the dependence of T_g on composition.[1,2] The pure-PEI assumption leads to a unique determination of both the proton fraction, m_E, associated with the pure PEI phase and the fraction, f_{em}, of PEI protons in the mixed phase. These quantities are given by

$$m_E = f_i/(1 + f_i) \quad (5)$$

and

$$f_{em} = 0.5(1 - f_i) \quad (6)$$

An alternate assumption we can make in order to relate f_i to stoichiometry is an assumption of symmetry, namely, that both phases are mixed and each phase possesses half of the total protons. It then follows that, if the two phases are distinguishable, there will be one PEI-rich and one PBI-rich phase; moreover, the proton fractions of the minor components in each phase will be equal. We define the minor fraction to be f_{mi}. The relation between f_{mi} and f_i is

$$f_{mi} = 0.5(1 - f_i^{1/2}) \quad (7)$$

From eqs 6 and 7 we note that when f_i is near unity (the near-pure-phase case), f_{em} will be about $2f_{mi}$. This is a consequence of the difference in assumptions; i.e., in order to achieve comparable levels of mixing, the concentration of the minor component must be about twice as high when only one phase is mixed compared with the concentration when both phases are mixed. In Table II values for m_E, f_{em}, and f_{mi} are given where the experimental intercept of Figure 5 has been used in conjunction with the intercept determined for the physical mixture to determine f_i's, and these, in turn, have been substituted into eqs 5–7.

In Table II the f_{em} and f_{mi} values become monotonically smaller with increasing heat treatment temperature. This trend would be expected if the development of phase stoichiometry were arrested by the vitrification of the PBI-rich phase. However, at 340 °C f_{em} is only 0.16, implying that the stoichiometry of the PBI-rich phase is very much dominated by PBI; only modest losses in PEI content are possible at higher annealing temperatures. Table II also includes the DSC-determined[2] T_g's associated with blends whose PEI proton fractions are given by the f_{em} values. According to this measure, an annealing temperature of 340 °C yields a PBI-rich phase whose composition is characteristic of a DSC-determined[2] T_g of about 400 °C. Perhaps this can be understood in terms of the difference in time scales between the DSC measurements (DSC sweep rates of 10–25 °C/min were chosen to reduce the influence of phase separation) and the 1-h time scale of annealing. Thus, while the high T_g of the PBI-rich phase is probably an important consideration in the limitation of domain growth, the stoichiometry of the PBI-rich phase cannot be so easily predicted from a DSC-determined T_g versus composition plot.

In Table II we have also included some numbers relating to the 310 °C sample. As indicated before, all of these numbers are imprecise because most of the corresponding decay in Figure 5 has occurred within the first 6 ms of spin diffusion. The numbers which appear correspond to lines drawn in Figure 5 through this data. The f_{em} value at 310 °C is much more typical of what one might expect when phase separation is arrested by an increasingly-vitrified PBI-rich phase, but we emphasize again that this number is only an approximation.

We add a cautionary comment on the subject of determining stoichiometries from intercepts using a physical mixture as a reference, especially since the measured integrals which are plotted are truncated. Changes in the relative contributions to this integral (e.g., from protons of PEI, PBI, residual water, or residual DMAc) from sample to sample will affect the measured intercept. In addition, line-width changes will also influence the relative contributions. We were particularly fortunate in this case that for the four samples, the physical mixture and the three blend samples annealed at 340, 370, and 400 °C, line shapes were virtually identical. Moreover, great care was taken to eliminate water by heating the samples at 150 °C in vacuum, just prior to measurement. The effectiveness of drying was judged by the absence of a narrowed resonance in the Bloch-decay proton spectrum. All of the DMAc had previously been driven off in the blend samples at the annealing temperatures; moreover, the physical blend had never been exposed to DMAc. Thus, while stoichiometric information, in general, will be harder to obtain than MDD's (τ_{sd}* is, to a first approximation, not sensitive to small changes in the PEI, PBI, water, and DMAc contributions to the integral from sample to sample), we feel that the stoichiometric information in Table II, corresponding to the three samples just mentioned, is reliable within the model-related assumptions and the error limits given.

Table II
Comparison of MDD's and Stoichiometric Information Deduced from the Spin-Diffusion Data of Figure 5 for Those Heat-Treated Blends Which Showed Phase Separation[a]

HT temp (°C)	f_i[b]	m_E[c]	f_{em}[d]	f_{mi}[e]	T_g (f_{em})[f]
340	0.68 (5)	0.41 (2)	0.16 (3)	0.09 (2)	402
370	0.83 (5)	0.45 (2)	0.09 (3)	0.04 (2)	411
400	0.92 (5)	0.48 (2)	0.04 (3)	0.02 (2)	417
310	0.30[g]	0.23[g]	0.35[g]	0.24[g]	372[g]

[a] Error estimates, in units of the last decimal place, appear in parentheses; errors do not include the ±5% error in determining the intercept for the physical mixture since this error introduces a systematic uncertainty. [b] Ratio of the τ_{sd} = 0 intercept in the blend relative to that (=0.101) in the physical mixture. [c] Proton fraction of the pure-PEI phase assuming the other phase is mixed. [d] PEI proton fraction in the single mixed phase, assuming the other phase is pure PEI. [e] Proton fraction of the minor component in each mixed phase using a symmetric model for phase separation in a 50/50 (proton stoichiometry) blend; i.e., each phase represents half of the total protons. [f] Based on data in ref 2. [g] The entries for the 310 °C sample are only intended to be illustrative since no well-defined linear portion of the decay curves was observed.

Effects of Heat Treatment on Solubility. The PEI/PBI system is an interesting example of phase separation because of the interplay of kinetics and thermodynamics. Our concern in monitoring changes in solubility, before and after heat treatment, was to probe whether chemical processes such as cross-linking were significant as possible competing mechanisms for limiting the growth of domains.

Films of PEI, PBI, and PEI/PBI blends of all stoichiometries are soluble in DMAc, the solvent used to make the films. If one waits long enough, these films will dissolve at ambient temperature. PEI solutions are colorless, and PBI imparts a yellowish color to the solution. Ambient-temperature solubility stands in contrast to the conditions reported[2] for getting the as-received PBI into DMAc solution (boiling DMAc at 165 or 225 °C corresponding respectively to atmospheric pressure or the use of a pressure bomb). These films contain residual DMAc reported[2] in the range from 0.04 to 2.7 wt %; the percent is roughly correlated with PBI content, although sample thickness must also play an important role. Thus, it is quite reasonable that the greater solubility of the PBI film, relative to the as-received PBI, is a result of the existence of a small amount of DMAc in the former. A change in the CRAMPS spectrum of the 50/50 blend occurred with heating above 250 °C; this change is most likely associated with the loss of about 1% DMAc, an amount consistent with expectations for this blend stoichiometry.

We also checked on the solubility of three film samples, PEI, PBI, and the 50/50 PEI/PBI blend, each of which

was annealed under a slight partial pressure of N_2 at 370 °C for 1 h. During annealing the PEI became a viscous fluid at 370 °C and coated the inside of the glass tube. A coated section, open at both ends, was cut out of this tube and immersed in DMAc. The PEI dissolved quite readily in warmed DMAC, but the solution had a slight yellowish tinge, indicating some chemical degradation. After dissolution, the section of glass tubing was removed from the solution; however, a thin milky coating remained on the inner surface of the glass tube. This coating had no particular affinity for the glass and could be scraped off the inner surface; nevertheless, this coating would not fully dissolve in fresh, warmed DMAc. Thus we conclude that a very small amount of PEI undergoes chemical degradation and becomes insoluble in DMAc.

Dissolution of the heat-treated PBI film also required heating the DMAC. Most of the PBI went into solution; however, wispy threads of gellike residues remained swollen but undissolved. These threads had no mechanical strength in the sense that one could not lift them intact from the solution with tweezers. The solution had the usual yellowish color. In contrast to the mostly-soluble heat-treated PEI and PBI films, the heat-treated blend would not dissolve in boiling DMAc. The film swelled considerably, yet the swollen pieces maintained recognizable shapes and had the mechanical strength to stay intact when held in the air with tweezers. The color of the swollen pieces was amber, the color in the solid state more typical of PBI, and the surrounding DMAc solution was almost colorless. From this it is not clear whether the PEI component was still partially soluble; nevertheless, the important point is that, following heat treatment, a much larger fraction of the blend sample became insoluble compared to the corresponding insoluble fraction for the heat-treated homopolymers. The implication is that chemical reactions are occurring between PEI and PBI and that the products are less soluble in DMAc. Annealing-induced cross-links, especially between PEI and PBI, are thus highly suspected.

Discussion

From the results summarized in Table I, several points can be made. First, both methods indicate that the original blend is well mixed. Second, PEI and PBI are indeed incompatible at elevated temperatures, and the SAXS correlation lengths as well as the MDD's from NMR increase with higher annealing temperatures. The influence of annealing time on phase separation was only addressed by SAXS measurements on the 25/75 PEI/PBI blend using annealing temperatures above the reported[2] T_g (263 °C) of this blend. These SAXS data suggest that the production of the inhomogeneities happens within minutes and the dimensions of these fluctuations in electron density change only slowly after that. The SAXS and the NMR data together demonstrate the incompatibility of PEI and PBI at each elevated temperature where phase separation is kinetically allowed. Interestingly, the increase in scattering intensity upon annealing at 300 °C in the 25/75 blend is not consistent with the phase boundaries based on DSC data.[2] The latter show that phase separation in a 25/75 PEI/PBI blend should occur only above 332 °C. Relative to the temperature associated with any LCST which the PEI/PBI system might possess, we can only say that it must be less than 300 °C.

A comparison of this study with DSC studies[1,2] on these blends indicates that one must exercise caution in using the DSC measurements to predict phase separation upon annealing. Two observations relate to this point. First, the stoichiometry of the PBI-rich phase in the blend annealed at 340 °C shows a composition whose T_g, as measured by DSC, is about 60 °C higher. Second, the first indications of phase separation were seen by NMR at 310 °C for a blend composition where the DSC-measured[1,2] T_g was 344 °C. We believe this primarily reflects the difference in time scale between the DSC measurements (several seconds) and the annealing times (≈1 h). The presence of escaping, residual DMAc solvent (≈1% in the original blend) could also facilitate phase separation at annealing temperatures below T_g. However, the plasticizing effect of DMAc is estimated[2] to be about 15 °C/wt % DMAc. Thus the presence of DMAc is not the principal reason for phase separation below the DSC-determined T_g. One must certainly proceed with caution if one considers putting such a high-T_g material into long-time service at temperatures even 60 °C below the DSC-measured T_g. Slow phase separation seems likely.

An important result of these studies is the verification that heat treatment results in MDD's and SAXS correlation lengths which are small on the usual scale of dimensions (micrometers) resulting from the latter stages of phase separation.[20] The most obvious limitation to growth at temperatures below the T_g of PBI should arise from the production of kinetically frozen, PBI-rich phases. A second limitation is the influence of possible cross-linking. If the latter is important and happens early in the phase-separation process, then the domain sizes will be strongly influenced by the exact thermal history of heating during heat treatment. Although the sample tubes were introduced into an annealing oven already at the annealing temperature, heating rates for the 50/50 blend samples were relatively slow due to the partial vacuum in the glass tubes and the relatively poor thermal conductivity of the glass.

The low PEI content of the PBI-rich domains (Table II) along with the MDD's (Table I) suggests that the cross-linking rate is not capable of dominating the diffusion process in the early stages of phase separation. It is possible, however, that cross-linked PEI/PBI copolymers ultimately help to stabilize a given domain size. This could happen either if PEI/PBI cross-linked molecules migrate to interface regions or if they are preferentially generated at the interfaces, owing to the greater PEI/PBI proximity there. Coupled with the slower transport kinetics of the PBI-rich phase, these cross-linked molecules could build up in sufficient numbers to dominate the interface regions, thereby stabilizing a given morphology.

Cross-linking, of necessity, involves chemical changes, and one can try to get a crude estimate of the extent of cross-linking by looking for spectral changes. In going from 340 to 370 to 400 °C, the aliphatic region decreased in relative intensity by about 2% over each temperature interval, i.e., 1 in 50 methyl protons "vanished". If these aliphatic intensity changes are a result of cross-linking, then, based on a number-average molecular weight for PEI of 12 000 (DP = 20), average changes in the number of cross-links per molecule in going from 340 to 400 °C could become the order of unity. If cross-linking occurs preferentially at the interface, however, cross-link distribution may be very inhomogeneous.

The pure-PEI-phase model for the stoichiometry of the phases in samples annealed at 340 °C and above is more likely to be appropriate than the "symmetric" model. Unpublished DSC studies[7] of 50/50 blend samples annealed at high temperatures to induce phase separation and then cooled show that the T_g of the PEI-rich phase is very close to that for pure PEI while the T_g of the other

phase increases with annealing temperature and annealing time.

According to Table I, the SAXS correlation lengths and the NMR-determined MDD's are quite disparate, the correlation lengths being smaller by factors between 3.1 and 4.6. Both ξ and the MDD are measures which pertain to particular (and very different) morphological models. The model for ξ invokes a fixed surface area but random and aperiodic distances across domains; in contrast, the model for the MDD's in Table I is a periodic lamellar structure. Clearly, both models cannot represent the true sample morphology. Both the SAXS and NMR measurements have been carried out on the same four samples which were annealed at the higher temperatures; thus, we can return to each kind of measurement with the idea that SAXS and NMR data are complementary and, taken together, should, in principle, offer a more accurate picture of the morphology.

We start with the assertion that all of the samples are isotropic; i.e., there is no sample-wide preferential direction which relates to morphology. We tested for anisotropy using two 370 °C-annealed, 50/50 blend samples where the X-ray beam entered the samples either perpendicular or parallel to the film plane. SAXS scattering curves were identical; isotropy was supported.

The SAXS and NMR data will be most complementary if the primary origin of the SAXS scattering is the electron density difference between phases of differing *chemical* composition, where each of the phases has (we assume) a uniform electron density. Should it be true that electron density fluctuations could occur for other reasons, e.g., local stress concentrations developed upon cooling, then the SAXS measurements would be probing a different distribution relative to the distribution sensed by the NMR measurements. (It is a natural outcome of the method of line-shape analysis for the NMR spin-diffusion experiments that differences in chemical composition characterize the phases detected.) In the following paragraphs we present arguments which lead us to the conclusion that the SAXS scattering is dominated by electron density fluctuations over distances smaller than those characteristic of the phases; i.e., variations in chemical composition do not account for the greatest fluctuations in electron density. It is important to recognize that the overall SAXS scattering power is very weak in these samples, indicating that the electron densities of the homopolymer constituents are very similar.

The sample annealed at 340 °C plays an important part in this reasoning. The ξ value for this sample is 2.4 nm, while the MDD, assuming lamellar morphology, is 11.1 nm. There is no maximum in the observed SAXS scattering curve; therefore, there is no periodicity in the electron density fluctuations, i.e., no repeat distances having dimensions less than 40 nm, with the upper limit determined by the beam stop. Moreover, there is no hint that a maximum is hidden behind the beam stop., From the NMR data, the deduced lamellar MDD of 11 nm implies a repeat distance of 22 nm. The MDD associated with a given spin-diffusion decay curve like those of Figure 5 depends on the assumed morphology. The smallest possible MDD is associated with a lamellar morphology, and the largest MDD is associated with geometries having the MDD in all three dimensions, i.e., spheres. While spheres were dismissed as highly unlikely when phases of comparable volume fraction are expected, we did consider the two-dimensional case, i.e., a rod/matrix morphology. Numerical computer modeling of the spin-diffusion problem using idealized rod/matrix morphologies, with the rod centers positioned on a square or hexagonal lattice, showed that one would get very comparable spin-diffusion decays (equal initial slopes) when the distance between rod centers was 1.25 and 1.35 times the lamellar repeat distance (=2 × MDD) for the square and hexagonal lattices, respectively. For the 340 °C-annealed sample, this means repeat distances of 28 to 30 nm. Both the lamellar and the 2D models point to overall repeat distances within the range probed by the SAXS scattering. Yet there is not even a hint of a plateau in this region. Thus, if the SAXS and NMR data are to be reconciled as both arising from fluctuations in chemical composition, either the effective spin-diffusion coefficient has been grossly overestimated to give the disparity between the MDD and ξ or the spin-diffusion decay curves have to be argued to be consistent with a very wide distribution featuring many small domains. We comment on these possibilities now.

In order to narrow the disparity between the ξ and MDD values in Table II, one would require a reduction in the assumed spin-diffusion constants by an order of magnitude. This reduction would be ludicrous, especially since the Bloch-decay proton spectrum of the blend, taken with 4-kHz MAS, shows only weak spinning side bands, implying that MAS is not quenching spin diffusion. We also have entertained the possibility that D could effectively be reduced by the creation of cracklike voids at most of the interfaces. If the cracks were at least 0.5 nm wide, they would present a spin-diffusion barrier between phases so that the spin-diffusion paths would be more tortuous and hence give the impression that dimensions were larger. We have dismissed this possibility as being too costly energetically (vide infra) since a polymer–polymer interface will typically have a lower surface energy than a polymer–void interface. Also, evidence of such cracks should have been seen but were not observed in the SAXS data.

We now turn to the question of what kind of a distribution of MDD's can be tolerated according to the NMR data. Specifically we ask whether the observed portion of the interphase spin diffusion tells us anything about the distribution. Also, we consider what quantity of small domains could be masked via our inability to separate the intraphase and interphase spin diffusion at short times. Qualitatively, the presence of a distribution of MDD's, as opposed to a single MDD, produces a shorter linear region for each spin-diffusion curve. When the volume fraction of each phase is about 0.5, the computer modeling of the idealized periodic-morphology models yields linear behavior over approximately the first 65% and 55% of the decay curves (like those of Figure 5) for the lamellar and rod/matrix models, respectively. The lines drawn through the data of Figure 5 suggest approximate linearity of the decays over 40–50% of the range, although, admittedly, a reasonable fraction of the early decay is eclipsed by the intramonomer spin diffusion. While some curvature associated with interphase spin diffusion is certainly possible in this eclipsed region, the amount of early-time curvature (a measure of the prevalence of small domains) is limited by the intercept at 0.101 for the physical blend. A related consequence of invoking such early-time curvature is that the greater the curvature, the purer the phases become stoichiometrically. Since the linearly-extrapolated data already imply phases of surprising purity (see Table II), there is reduced incentive to argue for curvature in this eclipsed region. To summarize the above considerations, there is little room for the NMR data in the eclipsed region to indicate a dominance of domains whose MDD's lie in the range of

those inferred from the SAXS analysis. Moreover, assuming linearity in this eclipsed range, the total fraction of the linear decay suggests that the dispersion in MDD's is modest (approximately 0.5–1.5 times the quoted MDD's); thus, some evidence of a SAXS maximum or plateauing should have been seen in Figure 1 especially for the sample annealed at 340 °C. The fact that no SAXS evidence for repeat distances in the 10–40-nm range was seen implies that the SAXS scattering is not primarily sensing fluctuations associated with phase boundaries.

There is a final bit of evidence for the claim that electron density fluctuations in these blends do not all occur at phase boundaries. The blend annealed at 310 °C showed evidence of phase separation in the spin-diffusion experiments but showed no evidence of phase separation in the SAXS scattering. Given that the total integrated scattering intensity is proportional to the product of the volume fractions of each phase times the square of the difference in electron densities between each phase and given that the NMR data point to approximate stoichiometries of 25/75 and 75/25 PEI/PBI, the integrated scattering intensity in the 310 °C-annealed sample ought to be about 25% that of the 400 °C-annealed sample. Experimentally, it is about 10%, not 25%.

We now discuss possible reasons for electron density fluctuations other than those arising from the phases themselves. We have considered the following possibilities: (a) nonuniform distributions of absorbed water, (b) annealing-induced fluctuations in density in the high-T_g PBI-rich phase, (c) clustering of cross-linked molecules, and (d) density variations (including voids) which result from the differential contraction of two biocontinuous phases with very disparate T_g's. Possibilities a and b were eliminated experimentally by doing scattering measurements on phase-separated blends having different water contents and on a 370 °C-annealed PBI film. Possibility c is not likely to dominate scattering if there is vanishingly small electron density contrast between the homopolymers. Possibility d seems, in the absence of better alternatives, most likely to us even though we view what follows to be highly speculative.

The critical assumption made is that the two phases are interpenetrating or bicontinuous; i.e., each phase forms a three-dimensional, continuous architecture. This characteristic is expected, for example, in the early stages of spinodal decomposition.[21] It is typical that the thermal expansion coefficient is larger for a polymer above its T_g than below it.[22] Thus, as one cools an annealed blend, particularly in the temperature range between the T_g's of the two phases, a significant differential contraction will occur. If voids are produced, the PEI-rich (fluid) phase would likely have a density near that of the homopolymer. If, on the other hand, as recent measurements have demonstrated,[23,24] the nucleation of voids is strongly resisted in the absence of impurities, then very strong negative pressures (up to the order of 1 kbar) can develop with corresponding deviations of a few percent from normal densities. In other words, strong negative pressures can be generated within the liquid phase. However, so long as the PEI-rich phase is liquid, stresses on each phase should be hydrostatic and uniform, with the expected result that density fluctuations would be characteristic of the domain dimensions (in contrast to what, we believe, is observed). Exactly how these stresses exhibit themselves in the ambient-temperature samples, through density fluctuations on a scale significantly shorter than the MDD of the phases, is highly conjectural. Possibilities include density fluctuations at high-stress points where we imagine stress concentration takes place after the vitrification of the PEI-rich phase. Another possibility is the inducement of nonequilibrium interchain orientational ordering as a result of local stresses. In these latter scenarios, it makes sense that the ξ values should progress in a way roughly proportional to the MDD values. Since the larger MDD values are associated with the higher annealing temperatures, the larger ξ values could either reflect the greater stresses associated with the larger range of cooling between the annealing temperature and the T_g of PEI and/or reflect the larger volumes of stress concentration when the characteristic dimensions of the glassy phase are scaled up. As a qualitative comment consistent with the foregoing explanation, we judge from experience that the strength of the scattering is comparable to the scattering expected when the electron density contrast is only a few percent. As an aside, the generation of internal stresses upon cooling requires only that the high-T_g phase be continuous; i.e., the phases need not be bicontinuous. However, if the PEI-rich phase consisted of droplets, then the development of density fluctuations on a scale smaller than the MDD is harder to imagine.

Conclusions

A solvent-cast 50/50 blend of a poly(ether imide) and poly(benzimidazole) has been shown by SAXS and NMR spin-diffusion measurements to be intimately blended on the 2.5-nm scale. This characteristic is maintained throughout 1-h annealing cycles at temperatures up to and including 280 °C. At annealing temperatures at 310 °C and above, phase separation is observed by NMR. The onset of phase separation thus occurs at temperatures in the vicinity of the reported T_g for this blend, 344 °C. For this 50/50 blend it remains an open question at what temperature, if any, below 310 °C, is a single phase thermodynamically stable. Prior to this study, DSC results were only able to demonstrate phase separation above 344 °C for this blend composition.

Phase separation in this blend is expected to be influenced strongly by the vitrification of the PBI-rich phase, owing to the much higher T_g of PBI (420 °C) relative to that of PEI (220 °C). In this study we have validated that domain sizes in those phase-separated, heat-treated PEI/PBI blends remain small, i.e., of the order of tens of nanometers. It is unfortunate that there remains some ambiguity about the origin of the small dimensions of the phases formed; i.e., is it the sluggish kinetics of the PBI-rich phase or is it cross-linking? (Via simple solubility tests on heat-treated samples of the blend as well as pure PBI and PEI, it was ascertained that some cross-linking occurred in each of these samples; however, the most probable cross-link seemed to occur between PEI and PBI rather than between homopolymers.) Nevertheless, the limited growth of domains is certainly consistent with expectations in a kinetically controlled system.

The NMR-determined stoichiometry of the PBI-rich phase formed at a given temperature of annealing has an associated DSC-determined T_g which lies about 40–60 °C higher than the annealing temperature. Thus, one must be cautious about how one relates DSC data (T_g versus composition) to the stability of blend structure when kinetics rather than thermodynamics is preventing phase separation. We believe that the fast thermal ramping required for the DSC measurement, relative to the 1-h annealing time, is the principal explanation for the foregoing difference, rather than, say, the influence of residual ($\approx$1%) solvent in the initial stages of phase separation or the lowering of T_g, owing to small domains.

If the latter reason dominated, we would not have seen the beginnings of phase separation at 310 °C when the DSC-determined T_g is 344 °C. Application of the two types of measurement, namely, NMR spin diffusion and SAXS, to phase-separated blends has led to corresponding estimates of characteristic morphological dimensions. These are, respectively, the minimum domain dimension (MDD) and the correlation length, ξ. In measurements on the same samples, the ξ values were 3.1–4.6 times smaller than the MDD's. We have come to the conclusion that the most likely explanation for this disparity is that the MDD's are those determined by the phase structure and the ξ values are determined principally by density fluctuations within the phases. This should not be taken as a general comment on the two methods because a critical argument which has led us to this point of view is that the electron densities for PEI and PBI are nearly identical. This is not the general case.

To summarize the complementarity of the SAXS and NMR measurements, we believe that the lamellar MDD's of Table I give reasonable estimates of the true MDD's but that a more appropriate model of the morphology is one allowing for bicontinuous phases whose characteristic MDD's would be better estimated using the idealized 2D model. This does not imply that bicontinuous phases are two-dimensional; rather, from a diffusional point of view, the MDD characterizes about two of the three dimensions. In other words, a bicontinuous phase might have roughly circular cross-sections normal to those directions of phase continuity where characteristic distances are much larger than the MDD and where diffusion along such directions would be unimportant in producing spin equilibrium. These 2D models would give overall repeat distances approximately 2.6 (instead of 2.0) times the MDD's given in Table I. The distribution of the overall repeat distances in samples annealed at 340 °C and above is estimated from the NMR data to be modest, spanning a range of about 0.5–1.5 times the mean value.

We believe that the SAXS measurements sense electron density fluctuations which are a result of phase separation but which occur on a scale smaller than that of the phases themselves. These fluctuations probably develop as a result of the stresses generated when a liquidlike, PEI-rich phase contracts at a more rapid rate than the glassy, PBI-rich phase upon cooling through the range between the annealing temperatures and the T_g of PEI. It is critical to the argument for stress buildup that the phases be bicontinuous.

This study has also shown the power of multiple-pulse proton NMR methods for characterizing polymer blends, even blends of chemically similar materials. Not only were characteristic distances determined but also stoichiometric information was obtained. We emphasize again that the role the SAXS scattering played in this study is unique to this blend; however, it allowed us to argue for a bicontinuous morphology and the presence of significant internal stress in the phase-separated morphologies. Neither of these latter features could have been deduced independently from the data of either technique.

Acknowledgment. We thank Dr. Geoffrey B. McFadden of NIST for writing the source code and performing several numerical calculations modeling spin diffusion in various idealized morphologies. This modeling provided important background for relating the NMR data to morphological models.

References and Notes

(1) Lueng, L.; Williams, D. J.; Karasz, F. E.; MacKnight, W. J. *Polym. Bull.* **1986**, *16*, 1457.
(2) Choe, S.; Karasz, F. E.; MacKnight, W. J. In Contemporary Topics in Polymer Science. *Multiphase Macromolecular Systems*; Culbertson, W. M., Ed.; Pergamon: New York, 1989; Vol. 6, p 493.
(3) Grobelny, J.; Rice, D. M.; Karasz, F. E.; MacKnight, W. J. *Macromolecules* **1990**, *23*, 2139.
(4) Guerra, G.; Choe, S.; Williams, D. J.; Karasz, F. E.; MacKnight, W. J. *Macromolecules* **1988**, *21*, 231.
(5) VanderHart, D. L. *Makromol. Chem., Macromol. Symp.* **1990**, *34*, 125.
(6) Campbell, G. C.; VanderHart, D. L. *J. Magn. Reson.* **1992**, *96*, 69.
(7) Karasz, F. E., personal communication.
(8) Certain commercial companies are named in order to specify adequately the experimental procedure. This in no way implies endorsement or recommendation by NIST.
(9) Abragam, A. *The Principles of Nuclear Magnetism*; Oxford University Press: London, 1961; Chapter V.
(10) Rhim, W.-K.; Elleman, D. D.; Vaughan, R. W. *J. Chem. Phys.* **1973**, *59*, 3740.
(11) Andrew, E. R. *Prog. Nucl. Magn. Reson. Spectrosc.* **1972**, *8*, 1.
(12) Ryan, L. M.; Taylor, R. E.; Paff, A. J.; Gerstein, B. C. *J. Chem. Phys.* **1980**, *72*, 508.
(13) Caravatti, P.; Neuenschwander, P.; Ernst, R. R. *Macromolecules* **1985**, *18*, 119.
(14) Debye, P.; Bueche, A. M. *J. Appl. Phys.* **1949**, *20*, 518. Debye, P.; Anderson, H. R., Jr.; Brumberger, H. *J. Appl. Phys.* **1957**, *28*, 679.
(15) VanderHart, D. L.; Gutowsky, H. S.; Farrar, T. C. *J. Am. Chem. Soc.* **1967**, *89*, 5056.
(16) Naito, A.; Ganapathy, S.; McDowell, C. A. *J. Chem. Phys.* **1981**, *74*, 5393.
(17) Havens, J. R.; VanderHart, D. L. *Macromolecules* **1985**, *18*, 1663.
(18) Douglass, D. C.; Jones, G. P. *J. Chem. Phys.* **1966**, *45*, 956.
(19) Paul, D. R. *Polymer Blends*; Paul, D. R., Newman, S., Eds.; Academic Press: New York, 1978; Vol. I.
(20) Cahn, J. W. *Acta Metall.* **1966**, *14*, 1685.
(21) Cahn, J. W. *J. Chem. Phys.* **1963**, *42*, 93.
(22) McKenna, G. B. In Comprehensive Polymer Science. *Polymer Properties*; Booth, C., Price, C., Eds.; Pergamon: Oxford, U.K., 1990; Vol. 2, Chapter 10.
(23) Angell, C. A.; Qing, Z. *Phys. Rev. B* **1989**, *39*, 8784.
(24) Green, J. L.; Durban, D. J.; Wolf, G. H.; Angell, C. A. *Science* **1990**, *249*, 649.

Registry No. PBI (SRU), 25734-65-0; Ultem 1000, 61128-24-3; poly(phenylenedibenzimidazole) blends, 61128-46-9.